Personalized Cardiac Mechanics Simulations of a Patient with Non-Ischemic Dilated Cardiomyopathy

Joventino O Campos[1], Daniel K Almeida[1], Thaiz R Schmal[2], Marcelle C S B Vasconcelos[2], Rodrigo W dos Santos[1], Bernardo M Rocha[1]

[1] Federal University of Juiz de Fora, Juiz de Fora, Brazil
[2] University Hospital of Juiz de Fora, Juiz de Fora, Brazil

Abstract

Advances in computational modeling of the cardiac function have allowed increasingly realistic simulations and studies closer to clinical applications, such as personalized simulations. In these simulations, data from the patient's medical exams are used to build a personalized cardiac model that can be used for virtual testing, with the aim of providing more information about the patient for clinical decision-making. The present work performs simulations of cardiac electromechanical activity using a geometry of the heart that was reconstructed from magnetic resonance images of a patient with dilated cardiomyopathy. In addition, the model parameters were adjusted so that the results corresponded to the patient's ejection fraction. Measurements of pressure, volume, stress, and strain throughout the cardiac cycle are reported, showing the influence of the existence of fibrosis on cardiac mechanics.

1. Introduction

Advances in computational modeling of cardiac function have allowed for more realistic simulations and studies closer to clinical applications. Researchers in this area have sought to develop faster simulators using efficient numerical methods and parallel implementations, which enabled studies regarding the reliability of models through uncertainty quantification [1] and sensitivity analyses [2], parameter estimation [3] and personalized simulations [4, 5].

In personalized simulations, data from medical exams, such as electrocardiogram, echocardiography or magnetic resonance imaging are used to create a personalized model [6] that allows virtual testing with the aim of contributing to clinical decision-making.

In the context of patients with dilated cardiomyopathy (DCM), for example, the diagnosis is based primarily on the patient's left ventricular ejection fraction. DCM is a myocardial disorder characterized by chamber enlargement and impaired contractility, which may be triggered by myocarditis [7]. Furthermore, deciding whether a patient requires an implantable cardioverter defibrillator demands invasive tests such as electrophysiological studies. Therefore, computational models emerge as a tool that can offer support for decision-making while reducing the number of invasive procedures that the patient needs to undergo.

In this sense, this work presents a personalized simulation for a patient with dilated cardiomyopathy, showing the influence of fibrosis on mechanical quantities of the ventricles. This simulation is capable of assessing information on cardiac function in a non-invasive manner, providing additional information for healthcare professionals.

2. Methods

2.1. Patient report

This study is based on data from a 79-year-old female patient under follow-up at the cardiology outpatient clinic of the University Hospital of the Federal University of Juiz de Fora. Magnetic resonance imaging revealed severe dilated cardiomyopathy with ventricular dysfunction and an ejection fraction of 21%. Late enhancement sequences showed regions of moderate subepicardial fibrosis in the septal, basal-medial, and inferior-medial regions.

2.2. Cardiac mechanics

The deformation of cardiac tissue is described by the following equilibrium equation:

$$\nabla \cdot (\mathbf{FS}) = \mathbf{0}, \text{ in } \boldsymbol{\Omega_0}, \tag{1}$$

where $\mathbf{F}$ is the deformation gradient tensor, $\mathbf{S}$ is the second Piola-Kirchhoff stress tensor, and Ω_0 is the undeformed configuration. Given the boundary conditions and applied loads, the equation is solved to find the displacement field.

Tissue contraction is considered through a decomposition of the stress tensor into a passive and an active part:

$\mathbf{S} = \mathbf{S_p} + \mathbf{S_a}$, where the passive part $\mathbf{S_p}$ is obtained from the strain energy function Ψ as $\mathbf{S_p} = \frac{\partial \Psi}{\partial \mathbf{E}}$, where $\mathbf{E}$ represents the Green-Lagrange strain tensor.

The active part represents tissue contraction due to an active force generated at the cellular level. The active stress is assumed to be anisotropic and applied in the fiber direction as: $\mathbf{S_a} = \mathbf{T_{ref}} \mathbf{T_a} \mathbf{f_0} \otimes \mathbf{f_0}$, where T_a is a normalized active stress generated by a cellular model, T_{ref} is a scaling constant of the active stress, and $\mathbf{f_0}$ is the unit vector that defines the fiber direction in the undeformed configuration.

The passive behavior of cardiac tissue was represented by the transversely isotropic model proposed by Guccione *et. al* [8], with strain energy function given by

$$\Psi = \frac{C}{2}(e^Q - 1) + \frac{\kappa}{2}(J-1)^2, \tag{2}$$
$$Q = b_f E_{11}^2 + b_t(E_{22}^2 + E_{33}^2 + E_{23}^2 + E_{32}^2) + b_{fs}(E_{12}^2 + E_{21}^2 + E_{13}^2 + E_{31}^2),$$

where $J = \det(\mathbf{F})$, E_{ij} are the components of the Green-Lagrange strain tensor, C is a stress-scaling parameter, while b_f, b_t, and b_{fs} are parameters related to stiffness in the fiber direction, perpendicular to the fiber, and shear parallel to the fibers, respectively. The parameter κ controls the tissue compressibility.

The active tension developed in a cardiac cell was represented by an arrangement of a contractile element in series with an elastic element [9]. It can be written in terms of the time since cell depolarization t_a, the sarcomere length l_s, and a contractile element of length l_c:

$$T_a = \frac{l_s}{l_{s0}} f_{\text{iso}}(l_c) f_{\text{twitch}}(t_a, l_s) E_a (l_s - l_c), \tag{3}$$

where l_{s0} is the reference sarcomere length and E_a is the stiffness of the elastic element. The function f_{iso} describes the isometric tension, while the function f_{twitch} represents the relationship of the tension in the fiber to t_a and l_s. The size of the contractile element varies as follows:

$$\frac{dl_c}{dt} = v_0(E_a(l_s - l_c) - 1), \tag{4}$$

where v_0 is the sarcomere shortening velocity [9]. Figure 1(e) presents the active tension curve used in this work.

During the cardiac cycle, the surface of the ventricular endocardium is subjected to dynamic loading due to the time-varying pressure exerted by the blood in the chambers. This pressure in the ventricles was represented by the lumped parameter model described in [10]. The solution of this model gives the left ventricle volume, which can be used to find the pressure to be applied to the ventricular endocardium at each time instant. Figure 1(d) presents an example of a time-varying pressure applied to the left ventricular endocardium.

2.3. Numerical solution

The finite element method is applied to the problem using a variational formulation presented in [11], which considers the displacement field, pressure, and dilation as unknowns. The domain is discretized into tetrahedral elements with linear approximations for the displacements and constant approximations for the pressure and dilation. The pressure and dilation variables are solved at the element level using the static condensation procedure, which results in a nonlinear system in terms of displacement field. This problem is solved using Newton's method, in which at each iteration a linear system is solved using the LU decomposition method through the PETSc library [12].

2.4. Geometry

The patient's computational biventricular geometry was obtained by segmenting medical magnetic resonance images using the Segment software. The borders of the epicardium and endocardium of the left and right ventricles are segmented in each image of the series. The fibrosis identified in the cardiac tissue was also marked and considered in the geometry.

The segmented images are then used as input to a script[1] that generates the surfaces of the patient's biventricular geometry. These surfaces are then used to generate the tetrahedral finite element mesh using Gmsh, shown in Figure 1(a). The Laplace-Dirichlet rule-based algorithm was used to approximate the fiber orientation, which is shown in Figure 1(b).

2.5. Computational experiments

Two simulations of a full cardiac cycle were performed considering the presented biventricular geometry. The C parameter of the constitutive model and the T_{ref} parameter of the active tension were adjusted to reproduce the left ventricular volume at end-diastole and end-systole of the patient and, consequently, the patient's ejection fraction was also adjusted. The following parameters of the constitutive model were used: $C = 0.6$ kPa, $b_f = 6.6$, $b_t = 4.0$, $b_{fs} = 2.6$, $\kappa = 300$ kPa, and $T_{ref} = 90$ kPa. The parameters used in the circulatory model are the reported in [1].

The first simulation assumes the same properties throughout the tissue, while the second assumes that the fibrotic region has different characteristics. In this case, the tissue stiffness in the fibrotic region was assumed to be $10\times$ greater, resulting in $C = 6$ kPa, and the contractility of this region is assumed to be zero $T_{ref} = 0$, as proposed in [13]. The simulation results are compared in terms of longitudinal strain and fiber stress measurements.

[1] https://github.com/FISIOCOMP-UFJF/MyoMesh

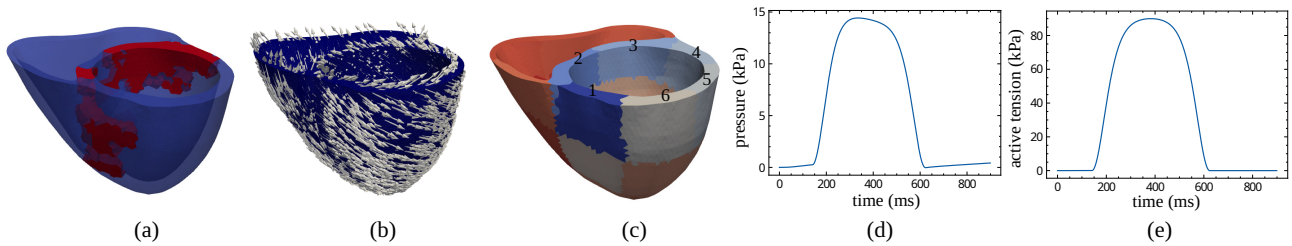

(a) (b) (c) (d) (e)

Figure 1. (a) Geometry reconstructed from medical images, with fibrosis marked in red. (b) Fiber orientation used. (c) Mesh parcelation according AHA segments used to compute stress and strain measurements. (d) Pressure applied to the left ventricular endocardium. (e) Active stress applied to each element of the domain.

As boundary conditions, zero displacement was imposed at nodes on the basal plane of the geometry. Furthermore, at each time step, a pressure value is applied to the surface of the left ventricular endocardium, as shown in Figure 1(d), and 20% of this pressure is applied to the endocardium surface of the right ventricle. The active tension shown in Figure 1(e) is applied to all elements at the same time instant, without considering the heterogeneity in cell activation throughout the cardiac cycle.

3. Results

The results of the two simulations performed are compared using pressure, volume, stress, and strain measurements. The simulation that assumes the same properties for the entire tissue do not consider the presence of fibrosis, while the case with fibrosis assumes different properties between healthy and fibrotic tissue.

Figure 2 presents the pressure-volume curve of the left ventricle for both simulations. The parameters of the simulation with fibrosis were adjusted to match the patient's data, which has an end-diastolic volume of $EDV = 251$ ml and an end-systolic volume of $ESV = 199$ ml, resulting in an ejection fraction $EF = 21\%$. For the case without fibrosis, it can be seen that the EDV increased and ESV decreased significantly, when compared to the fibrotic case with higher tissue stiffness and impaired contractility in the fibrotic region.

Longitudinal strain and fiber stress measurements were extracted throughout the cardiac cycle for segments of the mesh representing the basal segments of the American Heart Association (AHA) diagram, which can be observed in Figure 1(c). It can be seen in Figure 3 that the longitudinal strain magnitude throughout the cardiac cycle is significantly greater in the case without fibrosis. The curves are more synchronized in this case, as the contraction is homogeneous, and the negative peak is greater than the case with fibrosis, because all elements are able to contract. In the case with fibrosis, it is possible to see more dispersion in contraction, where the segments 3 and 4 presented low contraction, which is justified by the amount of fibrosis in these segments.

The fibrosis also impacts the fiber stress, where magnitude values decrease in this case, as shown in Figure 4. The reduction was greater in segments with more fibrosis than in segments where there is no fibrosis.

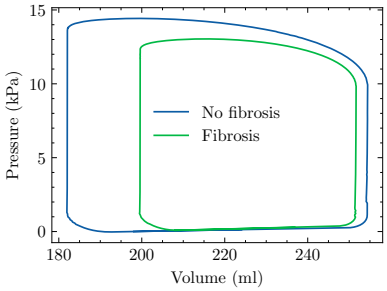

Figure 2. Pressure-volume relationship extracted throughout the cardiac cycle for the simulation considering homogeneous tissue (No Fibrosis) and for tissue with different properties for the fibrotic region (Fibrosis).

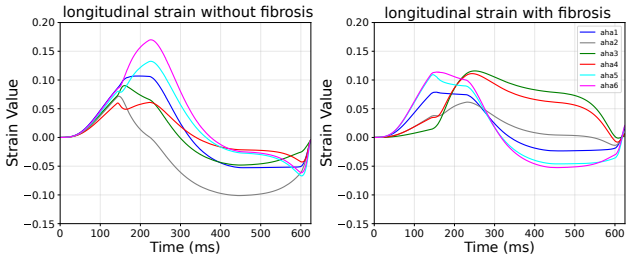

Figure 3. Longitudinal strain during the cardiac cycle for the six basal AHA segments of the left ventricle for the cases without and with fibrosis.

4. Conclusion

This study presented personalized simulations for a patient with dilated cardiomyopathy, where the presence of

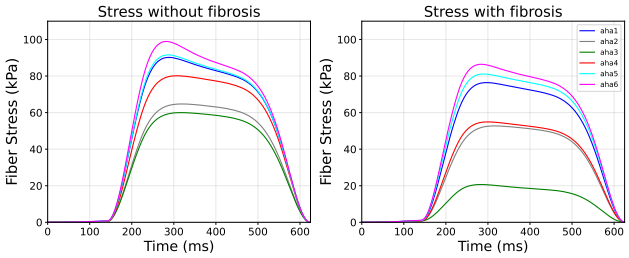

Figure 4. Fiber stress during the cardiac cycle for the six basal AHA segments of the left ventricle.

tissue fibrosis was evidenced by a decrease in the magnitude of tissue strain and fiber stress.

This approach demonstrates that personalized models can be used to assess conditions related to dilated cardiomyopathy through non-invasive procedures that can quantify ventricular dysfunction. Furthermore, new measurements, such as stress, which are difficult to obtain in medical examinations, can be calculated and used as markers for clinical decision-making.

Future work aims to calibrate the simulations so that the strain results correspond to the strain values obtained from the patient's echocardiography. This will then allow studying how markers computed from the model, such as stress, can aid in risk stratification for heart failure.

Acknowledgments

The authors would like to express their thanks to Minas Gerais State Research Support Foundation (FAPEMIG) - PCE-00048-25; APQ-02752-24; APQ-02445-24, "Coordenação de Aperfeiçoamento de Pessoal de Nível Superior" (CAPES), "Empresa Brasileira de Serviços Hospitalares" (Ebserh), "Conselho Nacional de Desenvolvimento Científico e Tecnológico" (CNPq) 423278/2021-5 and 301120/2025-0, and Federal University of Juiz de Fora (UFJF) for funding this work.

References

[1] Campos J, Sundnes J, Dos Santos R, Rocha B. Uncertainty quantification and sensitivity analysis of left ventricular function during the full cardiac cycle. Philosophical Transactions of the Royal Society A 2020;378(2173):20190381.

[2] Levrero-Florencio F, Margara F, Zacur E, Bueno-Orovio A, Wang Z, Santiago A, Aguado-Sierra J, Houzeaux G, Grau V, Kay D, et al. Sensitivity analysis of a strongly-coupled human-based electromechanical cardiac model: Effect of mechanical parameters on physiologically relevant biomarkers. Computer Methods in Applied Mechanics and Engineering 2020;361:112762.

[3] Campos J, Guedes R, Werneck Y, Barra L, dos Santos R, Rocha B. Polynomial chaos expansion surrogate modeling of passive cardiac mechanics using the holzapfel–ogden constitutive model. Journal of Computational Science 2023;71:102039.

[4] Scardulla F, Rinaudo A, Pasta S, Scardulla C. Evaluation of ventricular wall stress and cardiac function in patients with dilated cardiomyopathy. Proceedings of the Institution of Mechanical Engineers Part H Journal of Engineering in Medicine 2016;230(1):71–74.

[5] Camps J, Berg LA, Wang ZJ, Sebastian R, Riebel LL, Doste R, Zhou X, Sachetto R, Coleman J, Lawson B, et al. Digital twinning of the human ventricular activation sequence to clinical 12-lead ecgs and magnetic resonance imaging using realistic purkinje networks for in silico clinical trials. Medical Image Analysis 2024;103108.

[6] Soares TdJ, Pereira JPB, Werneck YB, Santos YRA, Franco TD, Campos JdO, Oliveira RS, Schmal TR, Souza TGSe, Rocha BM, et al. Studying arrhythmic risk with in-silico programmed ventricular stimulation and patient-specific computational models. In International Conference on Computational Science and Its Applications. Springer, 2023; 41–51.

[7] Imanaka-Yoshida K. Inflammation in myocardial disease: From myocarditis to dilated cardiomyopathy. Pathology International 2020;70(1):1–11.

[8] Guccione JM, McCulloch AD, Waldman L, et al. Passive material properties of intact ventricular myocardium determined from a cylindrical model. Journal of Biomechanical Engineering 1991;113(1):42–55.

[9] Bovendeerd PH, Kroon W, Delhaas T. Determinants of left ventricular shear strain. American Journal of Physiology Heart and Circulatory Physiology 2009;297(3):H1058–H1068.

[10] Shavik SM, Wall ST, Sundnes J, Burkhoff D, Lee LC. Organ-level validation of a cross-bridge cycling descriptor in a left ventricular finite element model: effects of ventricular loading on myocardial strains. Physiological Reports 2017;5(21):e13392.

[11] Campos JO, Dos Santos RW, Sundnes J, Rocha BM. Preconditioned augmented lagrangian formulation for nearly incompressible cardiac mechanics. International Journal for Numerical Methods in Biomedical Engineering 2018;34(4):e2948.

[12] Balay S, Abhyankar S, Adams M, Brown J, Brune P, Buschelman K, Dalcin L, Dener A, Eijkhout V, Gropp W, et al. PETSc users manual. Technical report, 2019.

[13] Willems E, Janssens KL, Dekker LR, van de Vosse FN, Cluitmans MJ, Bovendeerd PH. Strain-controlled electrophysiological wave propagation alters in silico scar-based substrate for ventricular tachycardia. Frontiers in Physiology 2024;15:1330157.

Address for correspondence:

Joventino de Oliveira Campos
Departamento de Ciência da Computação da UFJF, Juiz de Fora - MG, 36036-330
joventino.campos@ufjf.br